

1

2 ***CDeep3M* - Plug-and-Play cloud based deep learning for image**
3 **segmentation of light, electron and X-ray microscopy**

4

5 **Authors: Matthias G Haberl^{1,2}, Christopher Churas², Lucas Tindall¹, Daniela**
6 **Boassa¹, Sebastien Phan^{1,2}, Eric A Bushong¹, Matthew Madany¹, Raffi Akay¹,**
7 **Thomas J Deerinck¹, Steven T Peltier^{1,2}, Mark H Ellisman^{1,2}**

8

9

10 ¹ National Center for Microscopy and Imaging Research, School of Medicine, University of
11 California San Diego, Biomedical Science Building, 9500 Gilman Drive, La Jolla

12 ² National Biomedical Computation Resource, University of California San Diego, Atkinson
13 Hall, 9500 Gilman Drive, La Jolla

14

15

16 **Abstract**

17 As biological imaging datasets increase in size, deep neural networks are considered vital
18 tools for efficient image segmentation. While a number of different network architectures
19 have been developed for segmenting even the most challenging biological images,
20 community access is still limited by the difficulty of setting up complex computational
21 environments and processing pipelines, and the availability of compute resources. Here, we
22 address these bottlenecks, providing a ready-to-use image segmentation solution for any
23 lab, with a pre-configured, publicly available, cloud-based deep convolutional neural
24 network on Amazon Web Services (AWS). We provide simple instructions for training and
25 applying *CDeep3M* for segmentation of large and complex 2D and 3D microscopy datasets of
26 diverse biomedical imaging modalities.

27 **Main**

28 Biomedical imaging prospers as technical advances provide not only enhanced temporal¹
29 and spatial resolution but also larger field of views², and all at a steadily decreasing
30 acquisition time. Altogether an abundant amount of potential information can be extracted
31 from those very large and complex data volumes. In recent years, substantial progress has
32 been made using machine learning algorithms for image segmentation³. Three-dimensional
33 electron microscopy (EM) volumes, due to their extreme information content and increasing
34 volume size^{2,4}, are among the most challenging of segmentation problems and an area of
35 intense interest for machine learning approaches. To this end, different architectures of
36 deep neural networks⁵⁻⁸ show great promise towards one such challenge, the dense
37 segmentation of neuronal processes spanning terabyte volumes of serial electron
38 micrographs. However, generalized applicability of deep neural networks for biomedical
39 image segmentation tasks is still limited and technical hurdles prevent the advances in speed
40 and accuracy from reaching the mainstream of research applications. These limitations
41 typically originate from the laborious steps required to recreate an environment that
42 includes the numerous dependencies for each deep neural network. Further limitations arise
43 from the scarcity of high-performance compute clusters and GPU nodes in individual
44 laboratories, which are needed to process larger datasets within an acceptable timeframe.
45 With the goals of improving reproducibility and to make deep learning algorithms available
46 to the community, we built *CDeep3M* as a cloud based tool for image segmentation tasks,
47 using the underlying architecture of a state-of-the-art deep learning convolutional neural
48 network (CNN), DeepEM3D⁶, which was integrated in the Caffe deep learning framework⁹.
49 While there is a growing number of deep-learning algorithms, we were attracted to the
50 features offered by the CNN built in DeepEM3D⁶, as we recognized it to have advantages for
51 our applications, where both cellular and subcellular features are of interest. Specifically,
52 DeepEM3D is conceptually designed to be extremely broad in feature recognition with 18
53 million trainable parameters and three models trained in parallel on one, three and five
54 consecutive image frames giving excellent results for - but not limited to - membrane
55 segmentation⁶.
56 For *CDeep3M*, we modified all required components to make the CNN applicable for a wide
57 range of segmentation tasks, permit processing of very large image volumes, and automate
58 data processing. We also implemented a modular structure and created batch processing

59 pipelines, for ease of use and to minimize idle time on the cloud instance. Lastly, we
60 implemented steps to facilitate launching the most recent release of *CDeep3M* on Amazon
61 Web Services (AWS). To reflect the now broad applicability of our implementation to data of
62 multiple microscopy modalities (e.g., X-ray microscopy (XRM), light microscopy (LM) and
63 EM), we named this toolkit *Deep3M*. To give users easy access and to eliminate
64 configuration issues and hardware requisites, we further release a cloud-based version as
65 *CDeep3M*. The publicly available AMI (Amazon Machine Image) of *CDeep3M* can be readily
66 used for training the deep neural network on 2D or 3D image segmentation tasks. Using an
67 AWS account gives any user the immediate ability to spin up a machine with *CDeep3M*,
68 upload their training images and labels to generate their own trained model, and
69 subsequently segment their datasets. To make this useful for researchers with varying levels
70 of expertise, we minimized the number of sequential steps in *Deep3M* (**Fig. 1**), while still
71 allowing for flexible use of the code.

72 Here we provide complete instructions for how to go from training images to performing
73 segmentation using the deep neural network. Once the predicted segmentations are
74 accomplished they can be post-processed either using an already available script (see
75 supplemental material) or using standard image analysis and rendering tools (such as
76 ImageJ, IMOD, Amira etc.) to group and count objects, mesh surfaces, or perform further
77 analysis. We used *CDeep3M* for numerous image segmentation tasks in 2D and 3D, such as
78 dense neurite segmentation, cellular organelle segmentation (nuclei, mitochondria, vesicles)
79 or cell counting. We demonstrate the utility of this distribution of *CDeep3M* for LM, XRM,
80 multi-tilt electron tomography (ET) and serial block face scanning electron microscopy
81 (SBEM). Altogether this should facilitate the analysis of large scale imaging data and render
82 *CDeep3M* a widely applicable tool for the biomedical community.

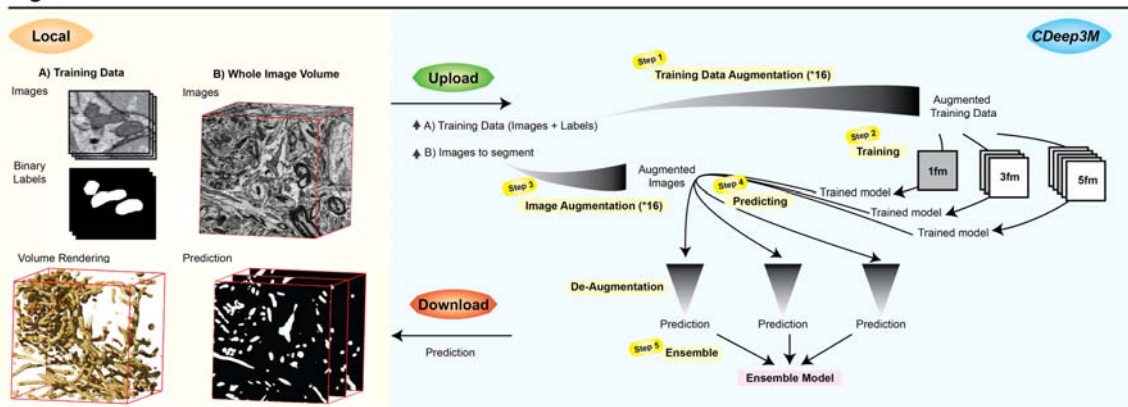
83

84 **Quick guide for using CDeep3M**

85 While pre- and post-processing steps are less computationally intense, we include the
86 necessary scripts in the pipeline on the same cloud environment for two reasons: first, to
87 provide all the steps required to run the entire processing pipeline without knowledge in
88 programming or the necessity to install or buy software and second, to minimize the traffic
89 to and from the cloud environment. Data augmentation during pre-processing (Steps 1 and
90 3) increases the training data volume substantially (>16-100 fold). Also, the segmented

91 results will be de-augmented in the post-processing (reducing it by a factor of up to a 100-
92 fold). Typically, transfer of data will be more time consuming and therefore expensive than
93 the added compute time on the cloud (<1min per 1000x1000x100 voxel). Steps 2 and 4 are
94 run sequentially for 1frame (fm), 3fm and 5fm for 3D datasets for improved accuracy,
95 whereas for 2D image segmentation only 1fm is run. Intense use of GPU occurs during steps
96 2 and 4 (training and prediction) requiring ~10GB of GPU memory at the current
97 configuration.
98

Figure 1



99

100 **Figure 1: Image segmentation workflow with *CDeep3M*.** Steps 1-2 are required to generate
101 a new trained model based on training images and labels. For 3D models *CDeep3M* trains
102 three different models (seeing 1 frame, seeing 3 frames and seeing 5 frames) that provide
103 three predictions (Step 4), which are merged into a single ensemble model at the post-
104 processing step (Step 5).

105

106 Data upload

107 It is necessary to upload training images and labels for steps 1-2 and raw data images for
108 steps 3-4. All images can be uploaded as folders containing sequential tif or png images or a
109 tif stack. Each will automatically be converted to the h5 file format during data
110 augmentation. Using the png file format is recommended to minimize the data transfer.
111 Training data consist of images and binary labels that use 0 as background and either 1 or
112 255 as positive label (see supplementary material for training data generation). A more
113 detailed description of individual commands, together with additionally implemented
114 scripts, is provided in the supplementary material. These scripts allow for more flexible use
115 of the processing workflow, for example, to re-use previously trained models.

116 Briefly, the cloud resource is accessed using the secure shell command (ssh). The secure
117 copy (scp) command is used to copy training images, labels, and image volumes to the cloud
118 (and to copy predictions back). *CDeep3M* learning and processing consists of 5 steps (see **Fig.**
119 **1**):

120 **Step 1: Preprocessing / Data augmentation of training images and labels**

121 `PreprocessTraining ~/train/images/ ~/train/labels/ ~/augm_train/`

122 **Step 2: Training *Deep3M* CNN (steps 2 and 4 run automatically for 1fm, 3fm and 5fm)**

123 `runtraining.sh ~/augm_tr/ ~/train_out/`

124 **Step 3: Preprocessing / Data augmentation of images to segment**

125 `PreprocessImageData ~/images/ ~/aug_images/`

126 **Step 4: Predict image segmentation (then performs data de-augmentation)**

127 `runprediction.sh ~/train_out/ ~/aug_images/ ~/predict_out/`

128 **Step 5: Ensemble prediction**

129 `EnsemblePredictions ~/predict_out/1fm ~/predict_out/3fm ~/predict_out/5fm ./ensemble`

130

131 **Examples**

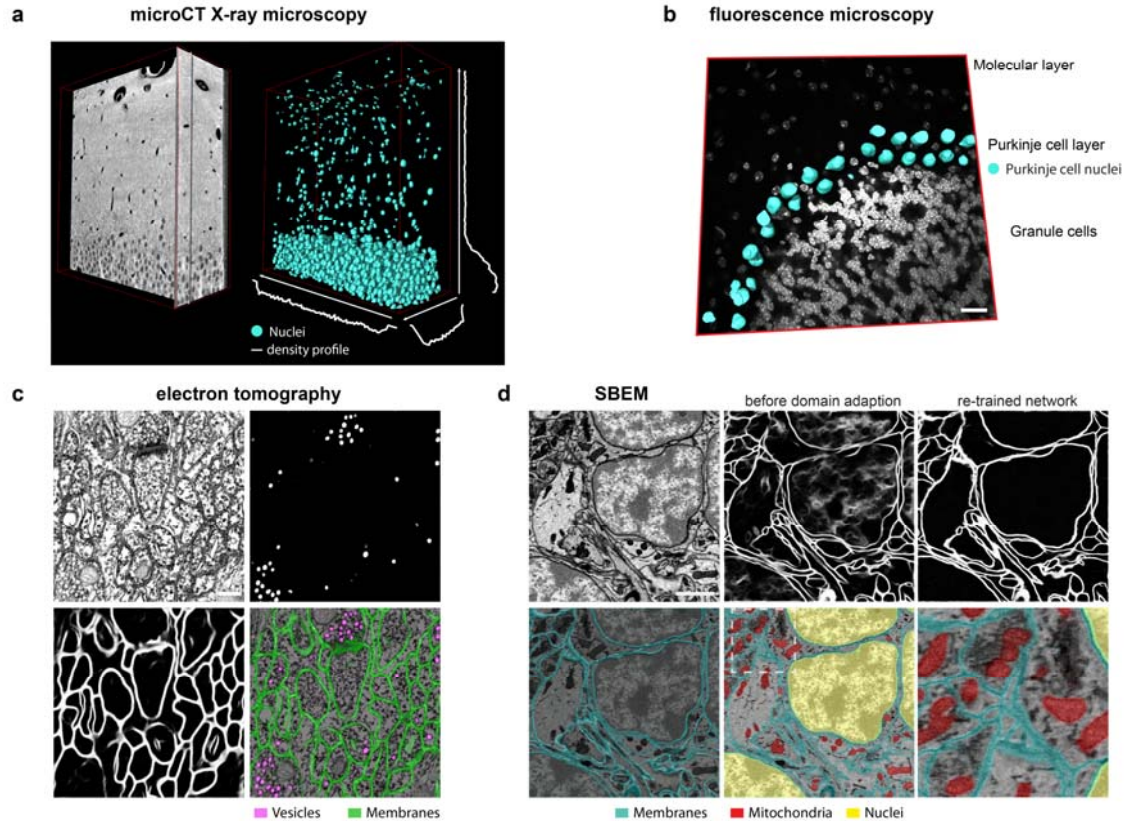
132 When training *CDeep3M* for the segmentation of nuclei in XRM data of a hippocampal brain
133 section, we established a cell density profile across the x-y-z directions of brain tissue
134 prepared for EM (**Fig. 2a**). Training on fluorescence microscopy images of DAPI stained brain
135 sections enabled us to distinguish neurons based on their chromatin pattern and distinguish
136 one individual cell-type from other cells in the tissue (**Fig. 2b**). Multi-tilt electron tomography
137 (ET) is a form of transmission EM used to achieve high-resolution 3D volumes of biological
138 specimens. Here, we applied *CDeep3M* to high-pressure frozen brain tissue and were able to
139 automatically annotate vesicles and membranes (**Fig. 2c**), which will aid the 3D
140 segmentation of synapses and neuronal processes. We further used *CDeep3M* for the
141 segmentation of intracellular constituents (nuclei, membranes and mitochondria) of the cell
142 in a serial-block face scanning electron microscopy (SBEM) dataset (**Fig. 2d**). For our
143 understanding of the role of intracellular organelles and alterations in diseases, parameters -
144 such as the precise volume, the distribution, and fine details like contact points between
145 organelles - will be of utmost importance. Therefore, we evaluated the performance
146 (precision, recall and F1 value) of the underlying CNN based on predictions per pixel, which
147 results in lower F1 values (compared to object detection) but is more representative to
148 determine accurate segmentations and distribution of intracellular organelles. We found the

149 segmentation accuracy of *CDeep3M* equals the one of human expert annotators
150 (**Supplementary Fig. 1**; *CDeep3M*: F1 value 0.9039, precision 0.9052, recall 0.9027; humans:
151 0.8827, precision 0.8993, recall: 0.8766).

152 Since training is time consuming and costly, both to generate manual ground truth labeling
153 and to train a completely naïve CNN, the re-use and refinement of previously trained neural
154 networks (transfer learning) is of eminent interest. Generating manual training data for
155 membrane annotation in SBEM is particularly laborious. To test our ability to re-use a pre-
156 trained model for a new dataset, we performed a type of transfer learning, domain
157 adaption¹⁰. We first trained a model on the recognition of membranes with a published
158 training dataset of a serial section SEM volume¹¹ (similar to ⁶) with a voxel size of 6x6x30 nm.
159 We then applied the pre-trained model to SBEM data with staining differences and novel
160 specific staining features (cellular nuclei) and with similar voxel size (5.9x5.9x40 nm). As
161 expected applying the network without further refinement on the new dataset lead to
162 unsatisfactory results (**Fig. 2d** (upper middle)). Adapting the histogram to better match the
163 earlier dataset and applying Gaussian de-noising to increase similarity between the two
164 image datasets was insufficient to remove the ambiguity of the prediction map introduced
165 by new features (nucleus) and staining differences. However, we found that re-training the
166 model with a short amount of training time (1/10th of the original training time) and
167 substantially smaller data size (1/5th) was sufficient to remove artifacts in the image
168 segmentation. Thus, we used only 20 training images and labels (1024*1024 pixel) instead of
169 100 and were able to adapt the network with 2000 or fewer iterations to the new dataset
170 (from 22000 to 24000 iterations for 5fm; **Fig. 2d**; 14454 to 15757 for 3fm; and 16000 to
171 18000 for 1fm, **Supplementary Fig. 2**). To distinguish nuclear membranes from the cellular
172 membranes, we performed separate training for the nucleus to distinguish the nuclei from
173 the cell somata (**Fig. 2d**). We hope that using existing models to greatly reduce the effort
174 required for training new models will encourage the community to share their trained
175 models and training data after publication. This could decrease the expense for image
176 segmentation by up to 90% (**Fig. 3**), making this an appealing approach even for smaller
177 segmentation tasks or when other image processing strategies may still be possible. For
178 users not deeply familiar with image segmentation operations, generating training data is
179 straight-forward (see supplementary material) and can be minimized for similar datasets.

180

Figure 2



181

182 **Figure 2: Multimodal image segmentation using CDeep3M.** (a) Segmentation of nuclei in
183 XRM volume of a 50µm brain slice containing the hippocampal CA1 area used for cell
184 counting and establishing a cell density profile across x-y-z. (b) Segmentation of cell type
185 specific DNA profile allows identification of Purkinje cells. Overlay of 3D surface mesh of
186 nuclei on light microscopic image of DAPI-stained cerebellar brain section. Scale bar: 20µm.
187 (c) Segmentation of vesicles and membranes on multi-tilt electron tomography of high-
188 pressure frozen brain section. Scale bar: 200nm. (d) Upper row: SBEM micrograph (left)
189 Scale bar: 1µm, segmentation using pre-trained model before (middle) and after domain
190 adaption (right). Lower row: segmentation of membranes, mitochondria and nuclei overlaid
191 on SBEM data

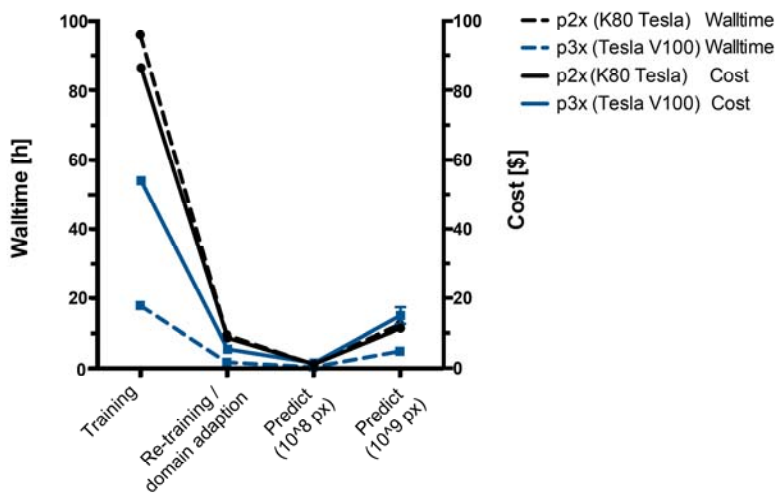
192

193 Discussion

194 To date, the prospect of paying per hour for compute devices might at first be less appealing
195 to members of the biomedical research community than the traditional one-time investment
196 approach. However, the requisite high-performance computers come at a high entry price

197 level. These resources are also outdated quickly and the maintenance of soft- and hardware
198 will, from our own experience, make cloud computing a more cost and time effective option
199 for most laboratories. We have further demonstrated ways to minimize costs for training
200 and expect prices for compute time to drop rapidly as newer GPU technology is developed.
201 Using cloud resources is scalable in times of high demand within the same laboratory and
202 free of cost and maintenance when unused. Our cloud-based solution to provide a public
203 AWS image is efficient for end-users, minimizing time spent for software / hardware
204 configuration, and alleviates the burden on algorithm developers to support a community
205 with a multitude of underlying systems and platforms. Furthermore, this will in the future
206 give end-users immediate access to any new release. Here, we demonstrate a flexible design
207 and ease of use that we expect will make the current release of *Deep3M* a useful tool for a
208 wide range of applications in cell biology.

Figure 3



209
210 **Figure 3: Time and cost evaluation.** Training expense can be reduced substantially (to
211 $1/10^{\text{th}}$) by performing domain adaptation from a pre-trained model (see **Fig. 2d** upper row).
212 The time for prediction scales linearly to the size of the imaging data. Time for prediction
213 and training both decrease with newer GPUs (Tesla V100 vs. Tesla K80). Cost calculations are
214 based on current rates at \$0.9/h for K80 and \$3.06/h for V100 instances.

215

216

217 **Data and software availability**

218 *CDeep3M* source code and documentation are available for download on GitHub
219 (<https://github.com/CRBS/cdeep3m>) and is free for non-profit use. Amazon AWS
220 cloudformation templates are available with each release enabling easy deployment of
221 *CDeep3M* for AWS cloud compute infrastructure. For the end user ~10 minutes after
222 creating the CloudFormation stack, a p2x or p3x instance with a fully installed version of
223 *CDeep3M* will be available to process data. Example data are available on GitHub and
224 trained models are available on Amazon S3. Further data will be made available upon
225 request.

226

227 **Author Contributions**

228 M.G.H. and M.H.E. conceived and designed the project. M.G.H., C.C. and L.T. and M.M.
229 wrote code and analysed data. M.G.H., D.B., S. P., E.A.B., T.D. performed experiments and
230 acquired images. M.G.H. and R.A. annotated training data. M.G.H., C.C., S.T.P. and M.H.E.
231 wrote the manuscript with feedback from all authors.

232

233 **Acknowledgments**

234 We thank Tao Zen for making DeepEM3D publicly available and for initial discussion. We
235 thank Dr. Silvia Viana da Silva for critical feedback on the manuscript. We thank Sung Yeon,
236 Nicolette M Allaway and Cesar Nava-Gonzales for help with ground truth segmentations.
237 Research published in this manuscript has received financial support from NIH grants
238 5P41GM103412-29 (NCMIR), 5P41GM103426-24 (NBCR) and 5R01GM082949-10 (Cell Image
239 Library (CIL). M.G.H. was supported by a postdoctoral fellowship from the interdisciplinary
240 seed program at UCSD to build a collaborative effort to map cells, called the Visible
241 Molecular Cell Consortium. This research benefitted from the use of credits from the
242 National Institutes of Health (NIH) Cloud Credits Model Pilot, a component of the NIH Big
243 Data to Knowledge (BD2K) program.

244

245

246 **References**

247 1. Chen, B. C. *et al.* Lattice light-sheet microscopy: Imaging molecules to embryos at high
248 spatiotemporal resolution. *Science* **346**, 6208 (2014).

- 249 2. Bock, D. D. *et al.* Network anatomy and in vivo physiology of visual cortical neurons.
250 *Nature* **471**, 177–184 (2011).
- 251 3. Long, J., Shelhamer, E. & Darrell, T. Fully convolutional networks for semantic
252 segmentation. *Proc. IEEE Comput. Soc. Conf. Comput. Vis. Pattern Recognit.* **07–12–**
253 **June**, 3431–3440 (2015).
- 254 4. Briggman, K. L., Helmstaedter, M. & Denk, W. Wiring specificity in the direction-
255 selectivity circuit of the retina. *Nature* **471**, 183–190 (2011).
- 256 5. Dorkenwald, S. *et al.* Automated synaptic connectivity inference for volume electron
257 microscopy. *Nat. Methods* **14**, 435–442 (2017).
- 258 6. Zeng, T., Wu, B. & Ji, S. DeepEM3D: approaching human-level performance on 3D
259 anisotropic EM image segmentation. *Bioinformatics* **d**, 2555–2562 (2017).
- 260 7. Januszewski, M. *et al.* Flood-Filling Networks. 1–11 (2016).
- 261 8. Lee, K., Zung, J., Li, P., Jain, V. & Seung, H. S. Superhuman Accuracy on the SNEMI3D
262 Connectomics Challenge. 1–11 (2017).
- 263 9. Jia, Y. *et al.* Caffe: Convolutional Architecture for Fast Feature Embedding. (2014).
264 doi:10.1145/2647868.2654889
- 265 10. Pan, S. J. & Yang, Q. A survey on transfer learning. *IEEE Trans. Knowl. Data Eng.* **22**,
266 1345–1359 (2010).
- 267 11. Kasthuri, N. *et al.* Saturated Reconstruction of a Volume of Neocortex. *Cell* **162**, 648–
268 661 (2015).
- 269